POSSIBLE LONG-TERM AND SHORT-TERM WIND PATTERNS INFERRED FROM MAPPING MARTIAN LARGE RIPPLES AND SAND DUNES. Z. Y.-C. Liu[1], J. R. Zimbelman[2], and L. K. Fenton[3], [1]School of Earth and Space Exploration, Arizona State University, Tempe, AZ 85287, USA (zacycliu@asu.edu), [2]Center of Earth and Planetary Studies, National Air and Space Museum, Smithsonian Institution, Washington, DC 20013, USA, [3]SETI Institute, Mountain View, CA 94043, USA

Introduction: Sand dunes and wind ripples have been extensively employed to derive surface wind patterns on Mars [e.g. 1-6]. Recent studies [6-8] have started to recognize possible long-term and short-term influences on the formation of dunes and ripples. Many studies [e.g. 1,4,5,9] have utilized various scales of numeric modeling, such as global scale Mars general circulation models (GCM), mesoscale models (e.g., Mars regional atmospheric modeling system, MRAMS), and microscale 3D airflow computational fluid dynamics (CFD) models, to analyze surface wind regimes based on aeolian features and compare the modeled winds with those derived from mapping of dunes and ripples. However, these results showed discrepancies between mapping-inferred winds and modeled winds. This may be in part due to the lack of recognition of different scales of winds and their influence on bedform construction (i.e. long-term vs. short-term). Since the knowledge of possible wind patterns in the long-term and short-term is essential to understanding past and present climate on Mars [4], this study aims to analyze the possible surface wind patterns derived from different aeolian features.

Methods: Here we adapt three techniques to derive surface wind regimes from mapping sand dunes and ripples. (1) Martian large ripples (LR): an approach previously developed by us [6], assuming the near-surface short-term wind is transverse to ripple crests. (2) IMGBNT (inverse maximum gross bedform-normal transport) $\boldsymbol{T_m} = \max\left(\sum_{i=1}^{N} \boldsymbol{Q_i} |\sin \alpha_i|\right)$ [5]: identifying the vector of maximum gross bedform-normal transport ($\boldsymbol{T_m}$) with bedform crest orientation (α) and inferring long-term sand transport $\boldsymbol{Q_1}$ from yardangs and wind streaks to invert possible sets of solution of wind transport vectors ($\boldsymbol{Q_2}$). (3) Dune slipface (DS) [e.g. 1-4]: assuming the long-term wind is transverse to dune slipfaces. We selected 10 study sites, which come from a wide range of topographic settings within a broad range of latitudes and longitudes around the planet (Table 1). We then compared the ripple-inferred winds (LR) in rose diagrams with those derived from both dune slipfaces (DS) and crestline alignments (IMGBNT) to examine the the degree of consistency of derived wind patterns.

Results: Fig. 1 shows the overall result of wind patterns drived from Martian large ripples using LR alignment in 10 selected mapping sites. In each study site at least one of the inferred winds is consistent with the orientation of a subset of the dune crestlines. Fig. 2 shows the mapping of LR and DS techniques in study site #9 and the corresponding wind roses. The wind comparison with three techniques in rose diagrams for study site #9 is shown in Fig. 3. $\boldsymbol{Q_1}$ transport vector is inferred from the unidirectional features (i.e., yardangs and wind streaks) around dune fields. Shaded areas in the IMGBNT rose diagram (Fig. 3) represents the possible solutions of wind transport vector $\boldsymbol{Q_2}$.

Discussions: Based on our mapping results, ripple-inferred wind regimes are generally consistent with either dune crestline orientations or IMGBNT winds. The former implies the interaction between airflow and dune crest topography (form-flow) [11], producing secondary flows (longitudinal to dune crestlines). This suggests LR alignment may indicate secondary flow patterns. Dune-constructing winds (i.e, those derived from IMGBNT) may better reflect large-scale, long-period wind dynamics. Large ripples may better reflect local-scale, short period wind dynamics (i.e., near-surface wind). DS alignment is less effective in dune fields constructed by multidirectional wind flows, which is in agreement with previous studies [e.g. 10]. Therefore, comparison of wind regimes using numeric modeling should be evaluated accordingly.

In addition, the mapping and wind results, especially from LR and DS techniques, may only represent a 'snapshot' of the most recent wind pattens. It is unclear if current winds are strong enough to move the sand and change the shape of ripples everywhere. That is, current wind regimes may not be consistent with dune and ripple derived winds. Thus, although dunes and ripples are the ground truth for flow circulation, they may not represent the current or paleo-wind regimes, given that the formation timescale of dunes and ripples are unknown for Mars. Comparsion with GCMs and mesoscale flow model should be used with caution.

References: [1] Hayward R. K. et al. (2007) *JGR, 112,* E11007. [2] Hobbs S. W. et al. (2010) *Icarus, 210*, 102-115. [3] Silvestro et al. (2011) *GRL, 38, L20201*. [4] Gardin E. et al. (2012) *PSS, 60(1),* 314-321. [5] Fenton L. K. et al. (2014) *Icarus, 230*, 47-63. [6] Liu Z.Y.-C. and Zimbelman J.R. (2015) Icarus, 261, 169-181. [7] Zimbelman J.R. and Ku Y.J. (2016) AGU, abstract EP21A-0858. [8] Ku Y.J. and Zimbelman J.R. (2017) LPSC this conference. [9] Jackson E.W. et al. (2015) *Nat. Comm. 6*. [10] Cardinale M. et al. (2012)

ESPL, 37.13, 1437-1443. [11] Walker I. J., and Nickling W. G. (2002) *Prog. Phy. Geo., 26(1),* 47-75.

Site	Region	HiRISE	Lon E	Lat
1	Gale crater	PSP_009571_1755	137.497	-4.463
2	Promethei Terra	ESP_022731_1080	143.002	-71.68
3	Aeolis Mensae	PSP_010178_1825	122.357	2.247
4	Ganges Chasma	PSP_008536_1725	314.784	7.409
5	Meridiani Terra	ESP_033483_1805	348.773	0.493
6	Near north polar	ESP_018525_2565	95.407	76.19
7	Coprates Chasma	ESP_031929_1660	296.815	-14.05
8	Near north polar	ESP_027739_2615	178.847	81.64
9	Wirtz Crater	ESP_021893_1315	334.676	-48.24
10	Near south polar	ESP_045311_1205	16.789	-58.97

Table 1. Location and HiRISE frame information for the 10 study sites. Sites are listed in order of completion, and they are spatially widely distributed around Mars (see Fig. 1).

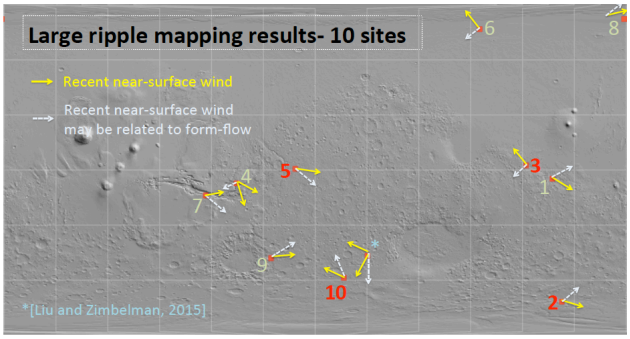

Fig. 1 The 10 mapping study site locations (Table 1) represented on a gray-scale MOLA elevation map. Arrows represent the near-surface winds inferred from LR alignment. White arrows represent the winds that may be related to form-flow interaction.

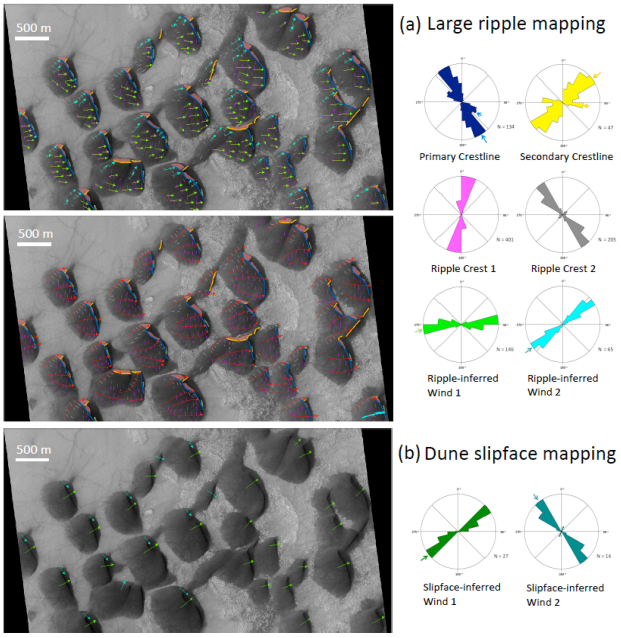

Fig. 2 (above) (a) Surface process map in HiRISE image ESP_021893_1315 (study site #9) with crestlines (dark blue and yellow), ripples (purple and gray), interpreted wind direction (green and light blue), and airflow (red), using technique of LR. (b) Surface process map using DS technique with slipface-inferred winds (green and blue).

Fig. 3 (below) Wind rose comparison of three wind-derive technique (IMGBNT, LR, and DS). Note that dashed-blue arrow in LR wind rose represent the possible form-flow, correlating with dune crestlines. In general, ripple-inferred wind regimes are generally consistent with IMGBNT wind solutions (***Q₂***).